The Journal of Experimental Biology 203, 2093–3004 (2000)
Printed in Great Britain © The Company of Biologists Limited 2000
JEB2525

THREE-DIMENSIONAL LOADING AND GROWTH OF THE ZYGOMATIC ARCH

KATHERINE L. RAFFERTY[1,*], SUSAN W. HERRING[1] AND FLAVIA ARTESE[2]

[1]*Department of Orthodontics, University of Washington, Box 357446, Seattle, WA 98195, USA* and [2]*Department of Orthodontics, Federal University of Rio de Janeiro, Brazil*

*e-mail: kraff@u.washington.edu

Accepted 10 April; published on WWW 22 June 2000

Summary

Despite a number of previous biomechanical studies on the zygomatic arch, unanswered questions remain about its three-dimensional loading and growth. Using young miniature swine, we have for the first time recorded strains from both the medial and lateral aspects of the squamosal bone during mastication and masseter muscle stimulation. Strains from the zygomatic bone flange and zygomatic arch growth data were also obtained from the same animals. A second study on a younger group of animals examined the growth of the zygomatic flange following partial removal of the masseter.

Strain data indicated that the squamosal bone is bent out-of-plane and that this pattern of loading is quite different from that of the adjacent zygomatic bone, which experiences much lower strains with little evidence of out-of-plane bending. Surprisingly, strains were higher in the zygomatic flange during contralateral chews and contralateral masseter stimulations than during ipsilateral chews/stimulations. These strains proved to arise from movement of the condyle, explaining why partial removal of the masseter had little effect on the growth of the flange. Other growth results indicated an approximately threefold greater rate of subperiosteal deposition on the lateral surface of the squamosal bone than on the zygomatic bone. This difference in growth rate is attributed to the presence of sutures that contribute to the lateral displacement of the zygomatic bone but not the squamosal bone. This explanation does not exclude the possibility that the rapid apposition on the lateral squamosal surface is regulated by the high surface strains that result from out-of-plane bending.

Key words: mastication, bone strain, bone growth, skull, miniature swine.

Introduction

Despite advances in techniques for studying *in vivo* biomechanics, our understanding of how the face and cranium are loaded during masticatory function is still largely incomplete. Unlike the postcranial elements, which provide opposing surfaces for the application of strain gauges, and thus at least the potential for resolving the three-dimensional loading, this is rarely true for elements of the craniofacial complex (but see Jaslow and Biewener, 1995; Throckmorton and Dechow, 1994, for *in vitro* studies of goat crania and human mandibular condyle, respectively). The focus of the present study, the zygomatic arch, is a beam-like structure, consisting of portions of the zygomatic and squamosal (temporal) bones, which spans the temporal fossa and thus provides the opportunity to measure strain on both the medial and lateral surfaces.

Although the zygomatic arch is now among the best studied of the bones of the craniofacial complex in terms of *in vivo* biomechanics, only the outer, lateral surface has been examined. Previous work in pigs (Herring and Mucci, 1991; Herring et al., 1996; Freeman et al., 1997) demonstrated strains of large magnitude in the zygomatico-squamosal suture and very different strain patterns in the zygomatic body and lateral squamosal components of the arch. An analysis of the trabecular architecture (Teng et al., 1997) found that anteriorly, in the zygomatic bone, the trabeculae were arranged primarily vertically and anteroposteriorly, whereas the posteriorly situated squamosal bone featured mostly mediolaterally directed trabeculae. The authors proposed that these architectural differences, together with differences in strain patterns (Herring et al., 1996), reflected bending of the anterior zygomatic bone primarily in the parasagittal plane (in-plane bending) and bending of the adjacent squamosal bone primarily in the transverse plane (out-of-plane bending). In a study on macaques (*Macaca fascicularis*), Hylander and Johnson (1997) found strain patterns that were generally similar to those observed for pigs. Although there was evidence for in-plane bending of the arch, they could not rule out the existence of simultaneous out-of-plane bending and twisting during mastication. They concluded that the zygomatic arch is ‘simultaneously bent in both the parasagittal and transverse planes and twisted about its long axis’ (Hylander and Johnson, 1997, p.239). Neither group was able to determine the relative importance of these different proposed loading regimes, largely because strain gauge

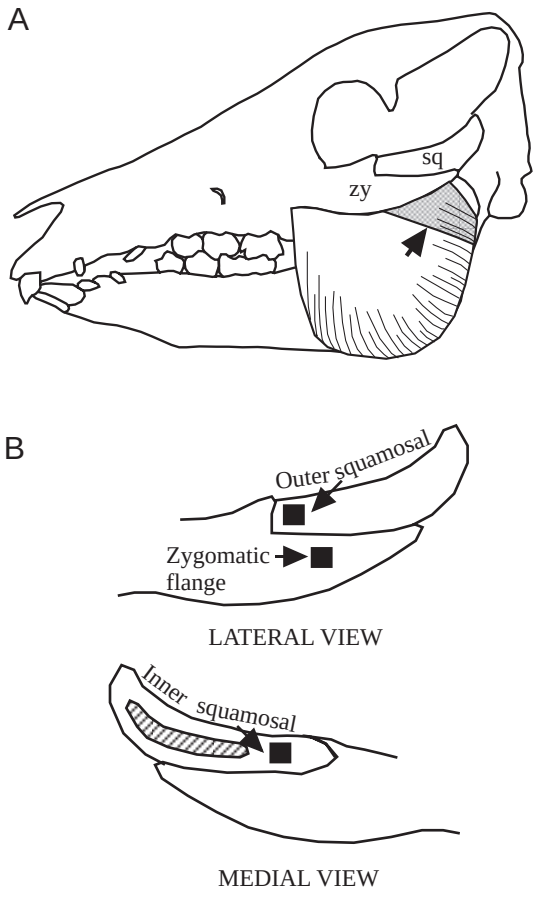

Fig. 1. Illustration of the zygomatic arch, masseter muscle and strain gauge locations. (A) Lateral view of a pig skull showing the location of the squamosal (sq) and zygomatic (zy) bones, and the position of attaching masseter muscle. The shaded area and arrow show the location of muscle fibers that were removed to test the hypothesis that growth of the zygomatic flange is in response to pull from the masseter. (B) Close-up of the zygomatic arch in lateral and medial view showing the location of rosette strain gauges. The hatched area in the medial view represents the articular eminence of the squamosal bone.

placement was confined to the lateral surface of the arch. Because the inner (medial) surface of the pig zygomatic arch is accessible, we have measured, for the first time, simultaneous strain in the medial and lateral parts of this element to determine the relative load contributions to the total pattern.

Strain studies on both pigs and macaques have found that the different portions of the zygomatic arch experience different strain magnitudes and orientations. However, the strain patterns in the posterior part of the zygomatic bone, known as the 'zygomatic flange', which lies inferior to the squamosal bone (Fig. 1), have not been investigated. Similarities in trabecular orientation between this part of the arch and the adjacent squamosal bone (compared with the anterior part of the zygomatic bone) led Teng et al. (1997) to suggest that its loading resembles the former more than the latter. In contrast, Herring (1993) previously proposed that the unusual zygomatic flange in pigs is a mechanical consequence of the attaching posterosuperior fibers of the masseter muscle, implying that these fibers are responsible for the loading and growth of the flange. We have now tested these opposing hypotheses: that the loading of the zygomatic flange is similar to that of the squamosal bone (on the basis of its architecture) or that its loading is consistent with the pull of the masseter (like that of the zygomatic body).

It is well known that mechanical factors play a role in the normal growth of the skull, as they do in the rest of the skeleton. However, the sparsity of information on *in vivo* loading of the face has hampered the study of how mechanical processes influence growth in this region. In models of adaptive modeling/remodeling, mechanical strains promote osteogenesis when they reach a certain threshold value (Frost, 1987) or when the daily strain stimulus (which includes both the magnitude and number of loading cycles) becomes sufficiently different from the attractor state (Carter et al., 1987). The resulting apposition, in turn, reduces the strains. Double fluorochrome labels given to the animals used for strain experiments allowed us to assess growth and microstructural differences in regions with different strain histories. A separate study examined the growth of the zygomatic flange in animals with intact and partially detached masseters. This study was designed as an explicit test of the hypothesis that the growth of the zygomatic flange of pigs is a mechanical consequence of the attaching posterosuperior fibers of the masseter (Herring, 1993). Information obtained from both these studies allowed us to examine whether patterns of growth (and microstructure) could be understood in a larger mechanical context.

Materials and methods

Strain and growth

Six male and six female Hanford strain miniature pigs (Charles River, Wilmington, MA, USA) were used for strain experiments. All experimental procedures were approved by the Animal Care Committee of the University of Washington. The animals ranged in age from 3.5 to 6 months and weighed 13.0–27.0 kg (Table 1). Rosette strain gauges (1–2 per subject) were placed on three locations on the left zygomatic arch: the inner (medial) and outer (lateral) surfaces of the squamosal bone just posterior to the vertical portion of the zygomatic suture, and the 'flange' of the zygomatic bone, which lies inferior to the squamosal bone (Table 1; Fig. 1). To determine which regions of the zygomatic arch were growing, double fluorochrome labels were given to the subjects prior to surgery and data collection. Calcein (Sigma, St Louis, MO, USA) was given *via* intravenous injection 7 days prior to the strain experiment (12.5 mg kg^{-1} calcein in a 5 mg ml^{-1} solution of pyrogen-free water neutralized with a 1 mol l^{-1} solution of NaOH and forced through a 0.22 μm syringe filter). A similar procedure was carried out with the second label, demeclocycline (Sigma) which was given 5 days later in a neutralized and filtered solution (15 mg kg^{-1} demeclocycline in 10 mg ml^{-1} in water). Both calcein and demeclocycline bind

Table 1. *Mass and strain gauge locations for subjects of strain experiments*

Pig	Sex	Mass (kg)	Squamosal		Zygomatic flange
			Inner	Outer	
234	M	26	X	X	
235	F	23	X	X	
236	M	16	X	X	
237	M	18	X	X	
242	F	22	X		X
243	F	27	X		X
252	M	19			X
253	M	13			X
254	M	20			X
255	F	23			X
263	F	23			X
264	F	21			X

with Ca^{2+} on the surfaces of newly forming apatite crystals, thus labeling the bone undergoing mineralization during the period of exposure (Tonna et al., 1984). The labels can be distinguished because calcein fluoresces green, whereas demeclocycline fluoresces orange.

The subjects were anesthetized with halothane and nitrous oxide. An incision was made in the skin along the superior aspect of the zygomatic arch, and the skin flap was retracted inferiorly with two small vertical incisions. At each gauge site, a three-sided square of periosteum was incised and reflected to expose a window of bone. Access to the medial site required the temporalis muscle to be held away from the medial surface of the arch within the temporal fossa. The windows of bone were prepared by a succession of cautery (minimal), scraping, degreasing, conditioning, buffering and drying. Once the surfaces had been prepared, stacked rectangular rosette gauges (SK-06-030WR-120, insulated with M-coat 'A' and M-coat 'D', Measurements Group Inc., Raleigh, NC, USA) were glued in place using a thin layer of cyanoacrylate. The *in situ* orientation of the strain gauges was documented by using a protractor to measure the angle between the occlusal plane (established by placing a tongue depressor between the molars) and the ε_2 element of the gauges. ε_1, ε_2 and ε_3 are the three elements of each strain gauge. Strain gauge orientation was also confirmed *post mortem*. After verifying that the gauges were operational by achieving a balance (Measurements Group 2120A strain gauge conditioners/amplifiers), the periosteum and skin were separately sutured. The lead wires with attached plug were led from the wound and secured to a collar around the neck. A topical anesthetic (2 % procaine hydrochloride) was drizzled onto the incision, and an analgesic (buprenorphine hydrochloride) was given by intramuscular injection prior to the recording session.

After surgery but with the animals still under anesthesia, fine-wire electromyography (EMG) electrodes were placed in the bilateral masseter and temporalis muscles (method described in Herring et al., 1996). The subjects were allowed to wake up from anesthesia and were offered water and their normal diet of pig chow. EMG signals were led to high-impedance probes (model 7HIP5G, Grass, Quincy, MA, USA) and then to amplifiers (Grass 7P3C). The amplified strain and EMG signals were then converted to digital signals (MP100, Biopac Systems, Inc., Santa Barbara, CA, USA) and input into a Power Macintosh running Acqknowledge III (Biopac Systems, Inc.). Data were collected at a rate of 500 Hz. Strain and EMG signals were recorded for 10–20 min of mastication, and the subjects were then reanesthetized and placed in a prone position for muscle stimulations.

For stimulations, needle electrodes were placed posterosuperiorly and anteroinferiorly into the masseter on both sides. Tetani were produced by 400–600 ms trains of 3–5 ms pulses delivered at 60 pulses s^{-1} (model S48 and SIU, Grass), and voltages were adjusted to achieve supramaximal masseter contractions. Both bilateral and unilateral contractions were produced with the teeth in occlusion. As with the mastication portion of the experiment, strain data were recorded using the program Acqknowledge. In two of the pigs, 263 and 264, zygomatic flange strains resulting from masseter stimulations were recorded both prior to and following the surgical cutting of the attachments to the flange, namely the masseter and the zygomaticomandibularis muscle and the lateral portion of the jaw joint capsule. Thirty minutes before they were killed, the subjects were injected with 3000 units of heparin intraperitoneally. They were killed by intracardiac injection of pentabarbitol followed immediately by decapitation and carotid perfusion with 2–3 l of heparinized saline and then approximately 4 l of 10 % neutral buffered formalin.

The instrumented zygomatic arches were then removed from the formalin-fixed skulls and stripped completely of soft tissue. Samples were also removed from the zygomatico-maxillary, lacrimo-zygomatic and fronto-lacrimal sutures of pigs 263 and 264 (Fig. 2). All samples were stored in 70 % ethanol until they could be air-dried, trimmed, attached to plastic stubs with epoxy resin and sectioned at a thickness of 60–70 μm using a Leica SP1600 saw microtome. Several sections were made from each sample. After mounting under coverslips in Permount (Fisher, Pittsburgh, PA, USA), they were viewed using the fluorescent mode (wavelength 390–420 nm) of a Nikon Eclipse E400 microscope. The pattern of fluorescent labeling was examined in two locations of the zygomatic arch: anteriorly at the location of the medial and lateral squamosal gauges, and posteriorly at the location of the zygomatic flange. Sections of the squamosal and zygomatic bones were examined qualitatively for differences in patterns of growth. Bone growth was also assessed quantitatively by measuring the distance encompassed by the second label (demeclocycline) on the appositional surface. This growth measurement was defined as the distance from the edge of the first label (calcein) to the edge of the bone's surface (see arrows in Fig. 6B,C). For each arch, six linear measurements were taken, three each from the squamosal and zygomatic bones at 25, 50 and 75 % of their height (Fig. 2B). A micrometer slide was used for linear calibration, and NIH Image software was used to take

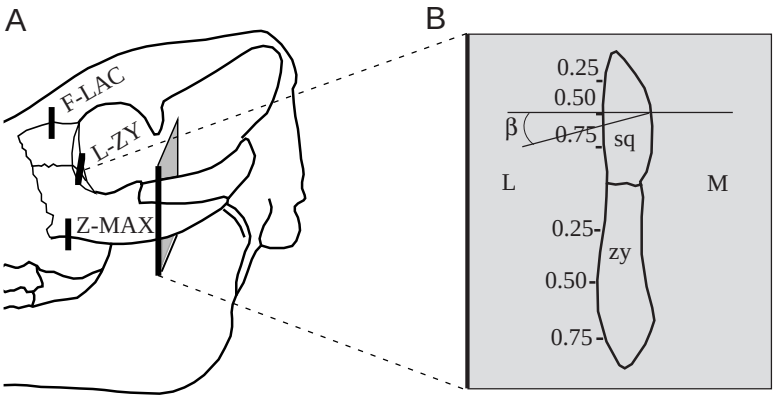

Fig. 2. (A) Lateral view of a pig skull showing the locations of sections through circumzygomatic sutures (bars). F-LAC, fronto-lacrimal; L-ZY, lacrimo-zygomatic; Z-MAX, zygomatico-maxillary. Sections were taken from a portion of the Z-MAX suture that is not visible in this view. (B) Close-up of the zygomatic arch in frontal section showing the squamosal bone (sq), the zygomatic bone (zy) and the six locations (given as a proportion of bone height) on the lateral surfaces of these bones where growth was assessed. Angle β is the orientation of the trabecular laminae in the squamosal bone. L, lateral; M, medial.

measurements from digitally captured images. The orientation of the trabecular laminae in the squamosal bone was measured from a horizontal line drawn perpendicular to the lateral edge of the squamosal bone at 50 % of its length (Fig. 2B). The sutural regions shown in Fig. 2A were chosen because growth in these areas would contribute to lateral growth of the face and thus lateral drift of the zygomatic arch. Given the small sample size for the sutural sample (N=2), growth at the zygomatico-maxillary, lacrimo-zygomatic and fronto-lacrimal sutures was assessed qualitatively.

Strain data were analysed by identifying recorded chewing sequences that appeared normal (e.g. 10–20 consecutive chews at 2–3 Hz) and then transferring the digitized waveform data of the power stroke portions of the masticatory cycles into Microsoft Excel. The baseline values were subtracted, and voltages were converted into microstrain. The principal strain magnitudes (ε_{MAX} and ε_{MIN}, tension and compression, respectively) and orientations were calculated from the three elements of each rosette strain gauge (algorithms provided in Tech Note 515, Measurements Group Inc.). The peak principal strains for each power stroke were identified as those coinciding with γ_{MAX}, the maximum shear strain ($\gamma_{MAX}=\varepsilon_{MAX}-\varepsilon_{MIN}$; Tech Note 515, Measurements Group Inc.), following the procedure of Hylander and Johnson (1989). The EMG pattern was used primarily to determine the side of chewing (see Huang et al., 1993). Given the characteristic square-shaped waveforms of the masseter stimulation data, only the mean value of the plateau region for each electrical burst (minus the baseline value) was extracted. The principal strains and orientations were calculated from these values.

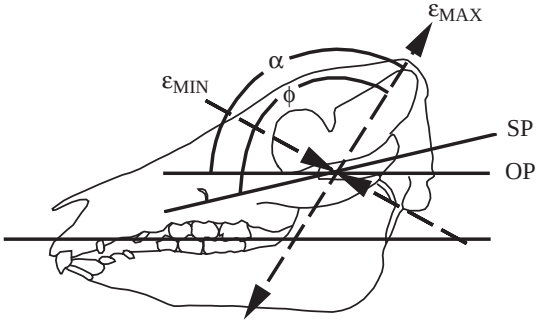

Fig. 3. Lateral view of a pig skull showing peak tensile principal strain (ε_{MAX}) and peak compressive principal strain (ε_{MIN}) at 90 ° to ε_{MAX}. Angles α and ϕ are measured between ε_{MAX} and the occlusal plane (OP) and to the squamosal plane (SP), respectively.

Two-sample t-tests were used to test for differences in strain magnitude (γ_{MAX}) between ipsilateral and contralateral chews and between ipsilateral and contralateral masseter stimulations. The orientation of the strain was calculated as angle α, a positive value measured from the occlusal plane to ε_{MAX}, the maximum (tensile) principal strain (Fig. 3). Individual mean angles and standard deviations and second-order analyses (the mean of mean angles) were calculated using rectangular coordinates, as described by Zar (1996).

The principal strains and orientations from the lateral and medial surfaces of the squamosal were broken down into longitudinal (ε_{long}) and shear (γ) strains, relative to the long axis of the squamosal. Because the squamosal plane is approximately 15 ° offset from the occlusal plane (Fig. 3), the angle α was first converted to ϕ, the angle measured from the squamosal plane to ε_{MAX}. Longitudinal strains from the lateral and medial surfaces were then used to calculate the bending (ε_B) and axial (ε_A) components of strain along the bone axis. The equations given below are from Carter (1978) and Carrano and Biewener (1999) (note that our equation for ε_{LONG} differs from that of Carrano and Biewener, which has a multiplication factor of 2, a typographical error; A. A. Biewener, personal communication):

$$\varepsilon_{LONG} = (\varepsilon_{MAX}\cos^2\phi) + (\varepsilon_{MIN}\sin^2\phi)\,, \quad (1)$$

$$\gamma = 2(\varepsilon_{MAX}\sin\phi\cos\phi) - (\varepsilon_{MIN}\sin\phi\cos\phi)\,, \quad (2)$$

$$\varepsilon_B = \pm(|\text{outer}\varepsilon_{LONG}|) - (|\text{inner}\varepsilon_{LONG}|)/2\,, \quad (3)$$

$$\varepsilon_A = (\varepsilon_{LONG}) - (|\varepsilon_B|)\,. \quad (4)$$

Partial masseter resection and growth

The growth experiment designed to test the hypothesis that posterior growth of the zygomatic flange is caused by tension from the attaching masseter muscle was carried out on a separate sample of six female Hanford miniature pigs (three pairs of siblings). All experimental procedures were approved by the Animal Care Committee of the University of

Table 2. *Peak principal strains during mastication*

Gauge site	Side	*N*	ε_{MAX} (με)	ε_{MIN} (με)	$\varepsilon_{MAX}/\varepsilon_{MIN}$	α (degrees)
Outer squamosal	C	4	570±251	−275±361	3.09±1.47	167±35
	I	4	780±350	−201±111	4.23±1.47	145±17
	C&I	4	682±302	−232±179	3.72±0.25	157±25
Inner squamosal	C	5	223±131	−636±255	0.36±0.16	96±13
	I	5	228±113	−552±269	0.42±0.09	115±21
	C&I	6	220±109	−572±238	0.39±0.10	106±18
Zygomatic flange	C	6	214±113	−241±110	0.90±0.19	69±34
	I	6	115±34	−162±77	0.87±0.44	65±24
	C&I	8	142±69	−168±85	1.03±0.48	56±30

Values are means ± S.D.

C, contralateral; I, ipsilateral; C&I, combined sides; ε_{MAX}, peak tensile principal strain; ε_{MIN}, peak compressive principal strain; α, strain angle.

Washington. On arrival at the age of 2 weeks, one member of each sibling pair was randomly assigned to the experimental group, the other to the control group. At the time of surgery (approximately 3 weeks of age), all pigs received a series of metal markers implanted in the squamosal and zygomatic flange. However, in the experimental group only, the muscular attachments to the zygomatic flange were completely resected bilaterally. The growth of the zygomatic arch was documented radiologically every 2 weeks over a 2-month period, during which time the animals quadrupled in body mass. At the end of this period, the animals were killed, and it was established through dissection that the posterosuperior fibers of the masseter had not regenerated in any of the three experimental animals. Measurements of the size and shape of the zygomatic flange were made from the dissected arches, including the length along the horizontal portion of the zygomatico-squamosal suture from its junction with its vertical component to the caudal tip of the zygomatic bone. To control for differences in body size, a size index of zygomatic flange length to skull length was constructed.

Results

Strain and growth

Mastication

The rosette data from the squamosal and zygomatic bones collected during *in vivo* function are presented in Table 2. Fig. 4 depicts the average principal strains and their orientations and Fig. 5 is a typical recording. The three locations showed distinctly different patterns of peak principal strain magnitudes. In the outer squamosal gauge, the peak magnitude of tension was always greater than the absolute peak magnitude of compression, as seen in the large value for the

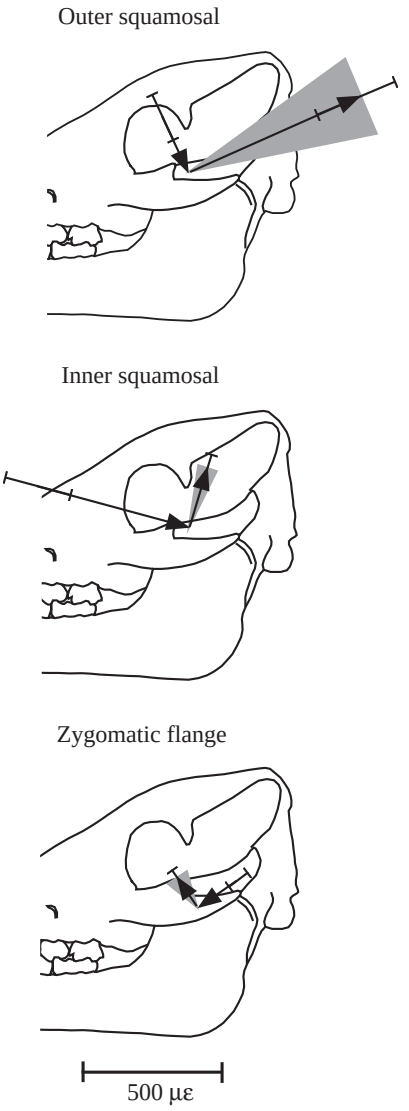

Fig. 4. Summary of the peak principal strains and their orientations at the three gauge locations. The length of the arrow indicates the magnitude of the mean peak principal strain, and the error bars indicate one standard deviation. The mean orientation is represented by the direction of the arrow, and the shaded area around the tensile principal strain indicates the standard deviation of strain orientation.

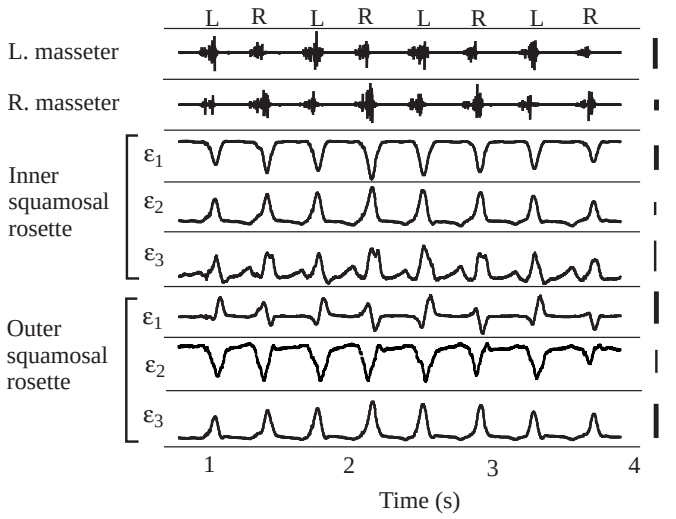

Fig. 5. Example of typical electromyogram (EMG) (top two traces) and rosette strain (bottom six traces) recordings. ε_1, ε_2 and ε_3 are the three elements of each rosette gauge. L and R at the top of the figure indicate chewing side (left or right). Thick scale bars, 0.5 V for EMG and 500 με for strain. Thin bars, 100 με. Data are from pig 236.

ratio of $\varepsilon_{MAX}/\varepsilon_{MIN}$ (mean 3.72). In contrast, the inner squamosal gauge of all pigs recorded absolutely greater compression, as seen by $\varepsilon_{MAX}/\varepsilon_{MIN}$ values of less than 1 (mean 0.39). The peak principal strain magnitudes were lower for the zygomatic gauge, and the ratio of $\varepsilon_{MAX}/\varepsilon_{MIN}$ varied around unity (mean 1.03). The inner and outer squamosal locations were significantly different from each other for $\varepsilon_{MAX}/\varepsilon_{MIN}$ (P=0.0002), but the zygomatic location was not significantly different from the outer squamosal location (P=0.07) (analysis of variance, ANOVA/Tukey test, combined side means).

The quality of the EMG recordings was insufficient to determine chewing side in two pigs, but results from the other animals suggested that the influence of chewing side varied with gauge location. The outer (lateral) squamosal gauges had higher ε_{MAX} values when the animals were chewing on the ipsilateral (left) side, significantly so in three out of four animals. In contrast, the inner (medial) squamosal gauge showed significant side differences in strain magnitude in one animal only. Like the outer squamosal location, strains in the zygomatic flange were affected by chewing side but, surprisingly, significantly higher strains were measured during contralateral (right) side chewing in four of the six pigs.

Each gauge location also had a distinct orientation of peak principal strains (Table 2; Fig. 4). In the outer squamosal gauge site, the average angle of 157° indicates that the peak ε_{MAX} was directed upwards and posteriorly (or downwards and anteriorly). The orientation of ε_{MAX} at the inner squamosal site averaged 106° relative to the occlusal plane. The orientation of ε_{MAX} at the zygomatic site was less than 90° in most pigs, indicating that, unlike the squamosal sites, ε_{MAX} is directed upwards and anteriorly (or downwards and posteriorly). Strain orientations at the three locations were significantly different from each other ($P \leqslant 0.02$; ANOVA/Tukey test).

The calculated values for longitudinal and shear strain at the medial (inner) and lateral (outer) squamosal gauge sites, and the overall axial and bending components, are presented in Table 3. The bending components were between 59% and 96% greater than the axial components, indicating that out-of-plane bending is a major loading regime. However, average shear strains were relatively high, and average shear [(inner γ + outer γ)/2] greatly exceeded bending (ε_B) in two pigs, 235 and 237 (which showed a value of 34° for ϕ in the outer squamosal site, approaching the expected value for torsion of 45°). Thus, twisting is also an important loading regime in some pigs.

Masseter stimulation

Results for masseter muscle stimulations in anesthetized pigs are presented in Table 4. As during mastication, the outer squamosal gauge site experienced a large tensile strain, whereas the inner squamosal site was under net compression (compare the mean $\varepsilon_{MAX}/\varepsilon_{MIN}$ values). Ipsilateral and bilateral masseter contractions produced strain patterns that were most similar to masticatory strain patterns at these two locations, although strain magnitudes were much higher for stimulation. Peak principal strain magnitudes at the zygomatic location were generally lower than those at the squamosal sites. Surprisingly, at the zygomatic flange, contralateral masseter stimulation produced strain magnitudes that were nearly equal to, or even higher than (in

Table 3. *Squamosal strains during ipsilateral chewing calculated from principal strains of the outer and inner squamosal surface (see Table 2)*

	Outer Squamosal			Inner Squamosal				
Pig	ϕ (degrees)	ε_{LONG} (με)	γ (με)	ϕ (degrees)	ε_{LONG} (με)	γ (με)	ε_A (με)	$\pm\varepsilon_B$ (με)
234	–17	984	712	–65	–416	646	284	700
235	–34	588	1269	–65	–319	500	134	454
236	8	663	237	–56	–572	1303	45	618
237	–34	198	388	–53	–215	479	9	206

ϕ, angle of the maximal strain (ε_{MAX}) relative to the long axis of the squamosal bone; ε_{LONG}, longitudinal strain; γ, shear strain; ε_A, axial component; ε_B, bending component.

Table 4. *Squamosal and zygomatic flange peak principal strains during masseter stimulation*

		Ipsilateral masseter				Contralateral masseter				Bilateral masseters			
Gauge site	*N*	ε_{MAX} (με)	ε_{MIN} (με)	$\varepsilon_{MAX}/\varepsilon_{MIN}$	α (degrees)	ε_{MAX} (με)	ε_{MIN} (με)	$\varepsilon_{MAX}/\varepsilon_{MIN}$	α (degrees)	ε_{MAX} (με)	ε_{MIN} (με)	$\varepsilon_{MAX}/\varepsilon_{MIN}$	α (degrees)
Outer squamosal	4	1451±869	−629±401	2.22±0.60	136±13	164±113	−83±64	2.27±1.30	189±22	1016±461	−368±100	2.71±0.85	139±12
Inner squamosal	6	280±186	−562±332	0.53±0.39	120±41	81±31	−178±81	0.46±0.11	91±13	192±101	−468±159	0.42±0.31	123±43
Zygomatic flange	7	116±125	−148±93	0.82±0.52	66±22	167±105	−152±127	1.55±0.87	57±42	86±37	−147±70	0.64±0.31	75±34

Values are means ± S.D.
ε_{MAX}, peak tensile principal strain; ε_{MIN}, peak compressive principal strain; α, strain angle.

three out of six animals), strain magnitudes produced by ipsilateral and bilateral contractions.

Because of the unusual finding that the contralateral masseter produced more strain on the zygomatic flange than did the ipsilateral masseter, we explored the possible sources of loading in the last two animals, pigs 263 and 264. First, zygomatic strains were measured before and after we progressively detached the masseter, the zygomaticomandibularis and the joint capsule (all but medial attachments) from the instrumented zygomatic arch. Removal of the soft tissues virtually eliminated the strains produced by ipsilateral masseter contraction, but the strains produced by contralateral masseter contractions were relatively unaffected. Second, we monitored strains while controlling movement. Strains produced by contralateral stimulations could be eliminated by firmly holding the teeth in occlusion. Furthermore, passive ipsilateral movements of the jaw (no muscle contractions) in the anesthetized animals produced strains in the instrumented zygomatic flange that resembled those of contralateral stimulation. Although these observations were qualitative and involved only two pigs, they clearly implicate movement as a source of strain on the flange.

Fluorochrome labels

Both locations showed the striking microstructural differences between the zygomatic and squamosal bones reported previously (Herring et al., 1996). The pattern of labeling in the zygomatic arch was similar in the anterior and posterior locations, but at each location the two bones were differently labeled. The zygomatic bone showed a compacting rim of bone surrounding a central region with large randomly oriented spaces (Fig. 6). Double fluorochrome labels were observed in the outer part of the cortical rim and lining the inner surfaces of the central spaces of the zygomatic bone. In contrast, the squamosal bone consisted of numerous thin laminae of bone that were discontinuous but strongly oriented in the mediolateral direction (Fig. 6). The labels were present as broad, diffuse regions on the surfaces of the bony laminae rather than clear bands paralleling the periosteal surface. Because of its much larger internal bony surface area, there was a greater amount of labeled bone in the squamosal than in the zygomatic bone.

Within each bone, the lateral surface showed a heavy concentration of label, indicating that it was undergoing apposition. In the case of the zygomatic bone, the borders of the lateral, inferior and most inferomedial surface were double-labeled, but most of the medial surface had either no label or a small amount of the second label (demeclocycline). The squamosal bone also showed a heavy lateral concentration of label, with the lateral-most laminae exhibiting only the second label and the medial surface generally showing no labeling. The medial surfaces of both bones exhibited occasional Howship's lacunae, which are indicative of resorption. Measurements of the distance encompassed by the second label on the lateral surface of the squamosal and zygomatic bones are presented in Table 5. Linear regression indicated that there were no consistent growth trends between anterior and posterior locations within the arch or from dorsal to ventral within each bone. Therefore, only mean values and standard deviations for all measurements from all locations/specimens for each individual are presented in Table 5. After the first

Table 5. *Growth and morphology of the zygomatic arch*

Pig	Trabecular angle, β (degrees)	Lateral growth (μm)	
		Squamosal	Zygomatic
242	26±1.0 (3)	346±63 (9)	118±18 (5)
243	30±3.5 (3)	335±44 (7)	104±42 (12)
252	38±2.1 (3)	387±34 (6)	–
253	32±0.5 (3)	238±55 (12)	110 (1)
254	30±3.3 (6)	463±83 (18)	139±4 (5)
255	27±3.7 (6)	661±89 (18)	174±28 (15)
263	25±0.6 (3)	291±26 (6)	115±15 (5)
264	26±1.0 (3)	541±20 (9)	139±23 (4)
Mean	29	408	128
S.D.	4.4	140	24

Values are means ± S.D.; values in parentheses are the number of locations measured.

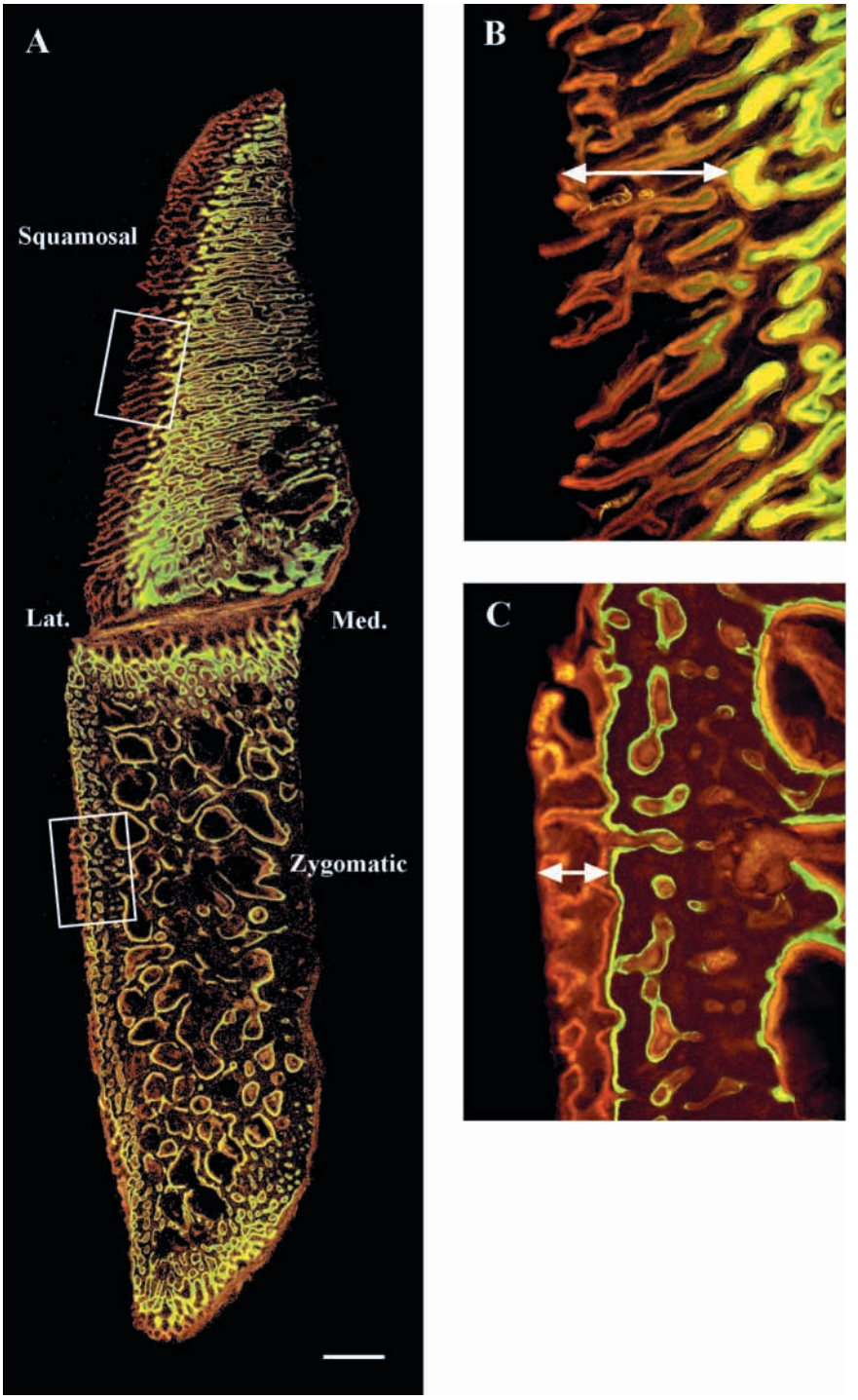

Fig. 6. Frontal section of a zygomatic arch viewed under ultraviolet light (see Fig. 2 for orientation). (A) Low-power view showing the squamosal and zygomatic bones separated by the horizontal part of the zygomatico-squamosal suture. Note that more bone is labeled (lighter regions) laterally (Lat.) than medially (Med.), and that the tissue is organized differently in the two bones. The squamosal bone consists of numerous thin, mediolaterally oriented laminae, whereas the zygomatic bone has large randomly oriented spaces in the central region, surrounded by a more compact outer rim. (B,C) Enlargements of the lateral borders of the squamosal (B) and zygomatic (C) bones, as indicated by the boxes in A. In the zygomatic bone (C), the double labels (red and green) mostly parallel the bone surface, whereas in the squamosal bone (B), the labels are oriented around the mediolateral laminae. The arrows indicate the distance between tne calcein-labeled region and the edge of the bone surface. This was used as an index of bone growth. Scale bar, 1 mm.

label had been completed, the lateral surface of the zygomatic grew, on average, 128 μm, whereas the squamosal grew more than three times faster, averaging 408 μm (P<0.01). The laminae of the squamosal bone were oriented at 29° from horizontal (see Fig. 2), indicating that this growth is lateral and slightly ventral in direction.

The circumzygomatic sutures were examined in only two individuals. However, examination of the zygomatico-maxillary, lacrimo-zygomatic and fronto-lacrimal sutures showed that all were double-labeled and were therefore growing actively. Growth was relatively low at the zygomatico-maxillary and fronto-lacrimal sutures (width of the second label approximately 20–30 μm), but apposition at the lacrimo-zygomatic suture actually exceeded that on the lateral surface of the zygomatic bone (approximately 150 μm compared with 127 μm of surface apposition in the same two animals, pigs 263 and 264). An additional interesting feature was the histological appearance of the fast-growing lacrimo-

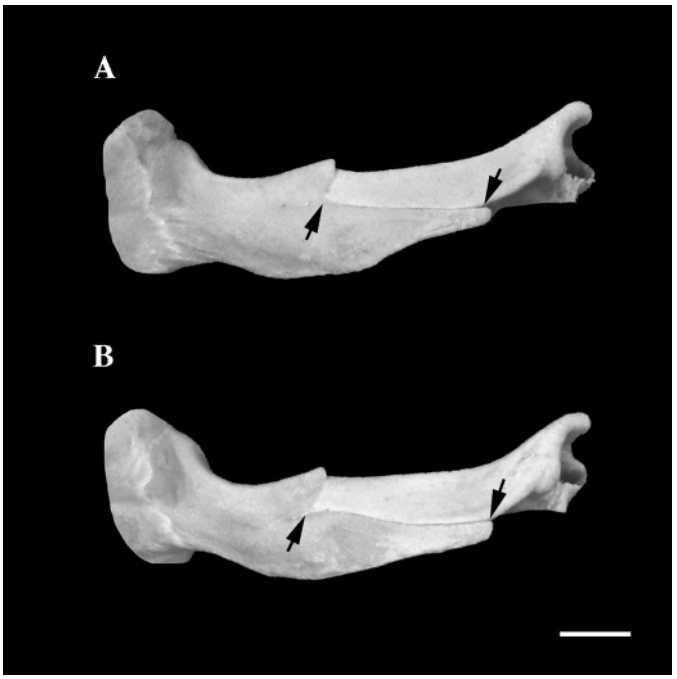

Fig. 7. Photograph of lateral views of pig zygomatic arches from the zygomatic flange growth study. (A) Two months after removal of the masseter fibers that attach to the flange (see Fig. 1A). (B) Control sibling (masseter intact). The distance between the arrows denotes the length of the zygomatic flange as measured by the length of the horizontal portion of the zygomatico-squamosal suture. Note that both flanges are of comparable length. Scale bar, 1 cm.

zygomatic suture, which exhibited a porous, chondroid-like structure. In a previous study, we interpreted this same morphology in the nasofrontal suture as being associated with both high compression and fast growth (Rafferty and Herring, 1999).

Partial masseter resection and growth

In the separate study on the growth of the zygomatic flange, the partial detachment of the caudo-dorsal fibers of the masseter muscle had no effect on the growth of the animals *in toto* or on the length of this part of the arch. The zygomatic flange size index (flange length divided by skull length) was 0.163±0.016 for the experimental group and 0.161±0.008 (means ± S.D., N=3) for the control group; these values are not significantly different (t-test). A visual comparison of the zygomatic flange from a pair of experimental and control animals is provided in Fig. 7. Clearly, the flange is fully developed in the experimental animal, although there may be some subtle differences in shape.

Discussion

Loading

The zygomatic arch has previously been instrumented with strain gauges in pigs (Herring and Mucci, 1991; Herring et al., 1996) and macaques (Hylander et al., 1991; Hylander and Johnson, 1997). In these studies, *in vivo* strains were measured from various locations on the lateral surface of the zygomatic arch (squamosal bone, zygomatic bone and the suture between them) using single-element and rosette strain gauges. These studies made it clear that the zygomatic arch is not a simple beamlike element, but were not able to determine the relative importance of shearing, torsion and out-of-plane bending. The present study confirms the previous findings from the lateral surface of the squamosal bone, except that the overall magnitude of strain in our pigs is considerably higher than that measured by Herring et al. (1996). The four animals with strain gauges on the outer squamosal bone (Table 1) were between 3.5 and 4.5 months of age and had an average γ_{MAX} value of 914 με during mastication and of 1451 με during ipsilateral stimulation. Masticatory and stimulations strains measured previously (Herring et al., 1996) were 411 με and 974 με, respectively. Two factors are probably responsible for this difference: (i) the pigs used by Herring et al. (1996) were older, on average, and (ii) the location of the outer squamosal gauge was slightly posterior to that used in the present study. Increasing stiffness with age and posterior position (the squamosal bone is thicker and better buttressed posteriorly) would translate into lower strain magnitudes.

New data from the medial surface of the squamosal bone clearly show that out-of-plane bending is a significant component of squamosal loading in pigs. The outer (lateral) surface of the squamosal bone is under substantial tension, whereas the inner (medial) surface is compressed. Thus, the bone becomes more convex on its outer surface and more concave on its inner surface. The source of this bending was speculatively assigned to the zygomaticomandibularis muscle by Herring et al. (1996). This may be the case, but a much simpler explanation is offered by an examination of the morphology of the zygomatico-squamosal suture (Fig. 8). The anterior vertical portion of the zygomatico-squamosal suture is beveled such that the zygomatic bone lies laterally and extends further posteriorly than the squamosal bone (Fig. 8). When the masseter muscle contracts, the zygomatic bone is pulled medially, posteriorly and inferiorly. In contrast, the squamosal portion of the zygomatic arch is fixed posteriorly to the cranium by the roof of the jaw joint. Contraction of the masseter puts the vertical portion of the zygomatico-squamosal suture under compression (Herring and Mucci, 1991). Because the zygomatic bone lies lateral to the squamosal bone at this suture, contraction of the masseter must cause the zygomatic bone to push down and back on the squamosal bone, bending it medially.

In addition to out-of-plane bending, the zygomatic bone of the pig arch may experience twisting about its long axis such that the lower border moves medially as a result of the medially directed component of masseter muscle force, whereas the upper border moves laterally. Such a deformation was proposed by Hylander and Johnson (1997) for macaques. Part of their argument for twisting of the arch was the observation that tension on the outer surface was oriented at approximately 45 ° from horizontal, posterosuperiorly for the squamosal and

Fig. 8. Photograph of a pig zygomatic arch in lateral view. The squamosal and zygomatic bones have been partly disarticulated to show the vertical component of the zygomatico-squamosal suture (arrow). Note that the squamosal portion of this suture lies medial to the zygomatic portion. Scale bar, 1 cm.

anterosuperiorly for the zygomatic bone. These orientations are similar in pigs (Herring et al., 1996). Further supporting the twisting interpretation in the macaque arch was the result that $\varepsilon_{MAX}/\varepsilon_{MIN}$ was nearly equal to 1.0 (Hylander and Johnson, 1997). Our finding of high shear strains suggests that the pig squamosal bone is loaded torsionally, but the finding of much larger tension on the lateral surface of the squamosal bone (mean $\varepsilon_{MAX}/\varepsilon_{MIN}$ 3.72) clearly rules out an interpretation of simple twisting.

Another interesting feature that argues against simple twisting is the strain pattern observed on the zygomatic flange. Because the gauge on the flange was located posterior to the squamosal gauges (Fig. 1), torsion should have caused a posterosuperior orientation of ε_{MAX}, just as for the squamosal bone. Indeed, we had expected to see similar strains in the flange and the squamosal bone because of some similarities in trabecular architecture (Teng et al., 1997). However, the results were quite different; ε_{MAX} in the flange was directed anterosuperiorly, as in the body of the zygomatic bone. This finding of separate loading regimes, regardless of position along the arch as a whole, implies that the zygomatico-squamosal suture acts to isolate the strain environments of the zygomatic and squamosal bones. Considered collectively, it seems likely that twisting is a less important form of loading in pigs than in macaques.

There are other differences between pigs and macaques in zygomatic arch strain patterns. Hylander and Johnson (1997) found that the lateral surface of the anterior portion of the macaque arch experiences much higher strains than the posterior portion (by a factor of three), whereas pigs experience larger strains posteriorly in the squamosal than in the zygomatic. The large anterior strains were interpreted by Hylander and Johnson (1997) to reflect in-plane bending resulting from an anteriorly concentrated masseter muscle. Such in-plane bending of the zygomatic bone has actually been documented in the zygomatic body in pigs, and the masseter muscle has been confirmed as its origin (Herring et al., 1996). The disparity between anterior–posterior strain magnitudes between the macaque and pig arch probably reflects the relative importance of in-plane and out-of-plane bending in these two groups. In contrast to the slender zygomatic arch of the macaque, pigs have a dorsoventrally deep arch, providing greater resistance to in-plane bending than to out-of-plane bending. Out-of-plane bending of the squamosal bone is responsible for the high posterior strains in the pig arch.

A final area of interest is the zygomatic flange, which is prominently developed in pigs. The most surprising finding about the zygomatic flange is that contralateral chews and contralateral masseter stimulations actually produced strains of larger magnitude than those produced by ipsilateral chews/stimulations or even bilateral stimulations. This result is unique in studies of the zygomatic arch, which have uniformly indicated that the ipsilateral masseter is the major source of loading. When we first observed this phenomenon, we hypothesized that stimulation of the contralateral masseter slightly displaced the condyle posteroinferiorly, causing the attaching tissues to put traction on the flange. In support of this idea is the observation that the ratio of tensile to compressive principal strain ($\varepsilon_{MAX}/\varepsilon_{MIN}$, Table 4) increased during contralateral stimulation, indicating a relative increase in tension compared with ipsilateral or bilateral stimulation. To test the hypothesis that soft-tissue stretching is the source of the load on the flange, strains were measured in response to stimulation of the masseter before and after attaching tissues were surgically cut. While the removal of the soft tissues virtually eliminated the strains produced by ipsilateral masseter contraction, the strains produced by contralateral masseter contractions were little affected. Therefore, the hypothesis of loads arising from soft-tissue traction was refuted. However, strains produced by contralateral stimulations could be almost eliminated by firmly holding the teeth in occlusion. Because this finding implicated movement rather than muscle pull as the source of strain, we then manipulated the jaw to deviate ipsilaterally in the direction of the instrumented arch (the same as the action of the contralateral masseter). Strains comparable with contralateral stimulations were produced. Therefore, there are two different sources that produce similar strains in the zygomatic flange: (i) contraction of the ipsilateral masseter, and (ii) ipsilateral movement of the jaw, which pushes the tissues lateral to the condyle against the zygomatic flange.

Growth and morphology

Two conclusions can be drawn from the qualitative and quantitative results on the fluorochrome labels: (i) both elements of the zygomatic arch grow laterally, dorsally and ventrally and (ii) the lateral surface of the squamosal grows more than that of the zygomatic. The first conclusion is completely understandable in the context of overall skull

growth. As the skull widens, the zygomatic arch must move laterally so as to maintain the space of the temporal fossa. In humans, and presumably in other mammals including pigs, this process involves lateral apposition and medial resorption (Enlow and Hans, 1996). In addition, the arch enlarges dorsoventrally through apposition at the horizontal part of the zygomatico-squamosal suture and at the dorsal and ventral periosteal surfaces of the squamosal and zygomatic bones, respectively. It is more difficult to understand how the lateral surfaces of these two contiguous bones could be growing at such different rates yet maintain their structural relationships. However, a resolution to the problem is suggested by considering the sutural environments of the two bones involved. The zygomatic bone can move laterally by displacement as well as by osseous drift. The zygomatico-maxillary, lacrimo-zygomatic and fronto-lacrimal sutures all have lateral components, so their growth displaces the zygomatic laterally. In contrast, the squamosal part of the arch is a continuation of the temporal bone and, therefore, can grow laterally only by direct apposition to its lateral surface.

In effect, the rapid subperiosteal deposition on the lateral aspect of the squamosal bone is necessary to maintain the structural/functional integrity of the arch as a whole as the zygomatic bone continues its lateral growth at the anterior sutures. This explanation for the differential growth rates also sheds light on the meaning of the microstructural differences between the squamosal and zygomatic bones. Within the squamosal, the bone is organized in a series of thin laminae oriented roughly mediolaterally. New bone continues to be added in this manner, i.e. roughly perpendicular to the periosteal surface, as opposed to parallel to the periosteal surface, as it is in the zygomatic bone. This laminar organization probably facilitates rapid subperiosteal growth, because a greater linear amount of bone can be added in the form of numerous fronds compared with the same amount of bone laid down more compactly. The measured angle of 29° can be interpreted as the actual direction of growth.

Although we interpret squamosal microstructure to be associated with rapid subperiosteal growth, this does not exclude the possibility that mechanical strains play a role in the regulation of squamosal modeling. According to Frost (1994), modeling drifts (which move the surfaces of a bone in tissue space) are ‘turned on’ in growing mammals by mechanical stimuli that reach some minimum effective strain. Most recently, Frost (1999) has suggested that this minimum effective strain range for modeling in young adults is 1000–2000 με. However, it is likely that not all parts of the skeleton have the same tissue sensitivity to mechanical stimuli, and the skull in particular may have a lower ‘set-point’ (Beaupré et al., 1990). A previous attempt to correlate modeling and strain in the cranial bones of macaques produced insignificant results, but was hampered by the fact that strains and modeling rates came from different animals (Bouvier and Hylander, 1996). The strains in the pig squamosal bone are large compared with those in other regions of the skull, including the zygomatic bone, and are unusual (for the skull) in falling into the range 1000–2000 με. It is important to note that other aspects of strain besides magnitude have known osteogenic effects, such as high strain rates and unusual strain distributions (Lanyon, 1996; Mosely and Lanyon, 1998) and total daily number of loading (strain) cycles (Mikic and Carter, 1995). Nevertheless, it is conceivable that the high strains on the squamosal bone have caused rapid apposition of bone, a process that would be halted only when the bone eventually consolidates into a cortex and strains decrease. Support for this suggestion in the previous finding of lower strain magnitudes in older animals is tempered by the fact that the strain gauge location was slightly different in these two groups of animals.

Finally, the strain analysis of the zygomatic flange explains the negative result of the experiment in which the posterosuperior fibers of the masseter muscle were detached. We had hypothesized that this would halt the elongation of the flange because tensile strain would be removed. No such inhibition of growth was observed. This surprising finding can now be seen to be due to an incorrect assumption about the origin of strain on the zygomatic flange. Our work indicates that the largest loadings are not of muscular origin but instead result from movements. Movements were unchanged in the experimental animals, and thus removal of the attaching muscle had little effect on the growth of the zygomatic flange.

Concluding remarks

In the present study, we took advantage of the construction of the zygomatic arch to provide the first glimpse of three-dimensional strain patterns in the skull. The data strongly support the importance of out-of-plane bending, accompanied by individually varying amounts of torsion, for the pig squamosal bone. The zygomatic flange, which is adjacent to the squamosal bone, is not involved in the bending and shows instead a strain pattern consistent with the pull of the masseter. Surprisingly, however, this strain pattern could be duplicated by jaw movements towards the zygomatic flange. This second source of strain may explain why growth of the flange is unaffected by removal of the masseter. Finally, a much higher rate of bone apposition was seen on the lateral surface of the squamosal bone than on the zygomatic flange. Although this growth differential is necessitated by geometric constraints, it is also correlated with the differential strain magnitudes experienced by the two bones.

This work was supported by PHS grant DE08513 from the National Institute of Dental Research. We thank Scott Pedersen, Zi Jun Liu and Christopher Marshall for their assistance with experiments and their helpful suggestions throughout the preparation of this manuscript. We also thank Trisha Emry for her help in the laboratory.

References

Beaupré, G. S., Orr, T. E. and Carter, D. R. (1990). An approach for time-dependent bone modeling and remodeling – Theoretical development. *J. Orthop. Res.* **8**, 651–661.

Bouvier, M. and Hylander, W. L. (1996). Strain gradients, age and levels of modeling and remodeling in the facial bones of *Macaca fascicularis*. In *The Biological Mechanisms of Tooth Movement and Craniofacial Adaptation* (ed. Z. Davidovitch and L. A. Norton), pp. 407–412. Harvard Society for the Advancement of Orthodontics. Birmingham, AL: EBSCO Media.

Carrano, M. T. and Biewener, A. A. (1999). Experimental alteration of limb posture in the chicken (*Gallus gallus*) and its bearing on the use of birds as analogs for dinosaur locomotion. *J. Morph.* **240**, 237–249.

Carter, D. R. (1978). Anisotropic analysis of strain rosette information from cortical bone. *J. Biomech.* **11**, 199–202.

Carter, D. R., Fyhrie, D. P. and Whalen, R. T. (1987). Trabecular bone density and loading history: Regulation of connective tissue biology by mechanical energy. *J. Biomech.* **20**, 785–794.

Enlow, D. H. and Hans, M. G. (1996). *Essentials of Facial Growth*. Philadelphia: W. B. Saunders Company.

Freeman, J. A., Teng, S. and Herring, S. W. (1997). Rigid fixation and strain patterns in the pig zygomatic arch and suture. *J. Oral Maxillofac. Surg.* **55**, 496–504.

Frost, H. M. (1987). Bone 'mass' and the 'mechanostat': A proposal. *Anat. Rec.* **219**, 1–9.

Frost, H. M. (1994). Wolff's law and bone's structural adaptations to mechanical usage: an overview for clinicians. *The Angle Orthodontist* **64**, 175–188.

Frost, H. M. (1999). Joint anatomy, design and arthroses: Insights of the Utah Paradigm. *Anat. Rec.* **255**, 162–174.

Herring, S. W. (1993). Formation of the vertebrate face: Epigenetic and functional influences. *Am. Zool.* **33**, 472–483.

Herring, S. W. and Mucci, R. J. (1991). *In vivo* strain in cranial sutures: The zygomatic arch. *J. Morph.* **207**, 225–239.

Herring, S. W., Teng, S., Huang, X., Mucci, R. J. and Freeman, J. (1996). Patterns of bone strain in the zygomatic arch. *Anat. Rec.* **246**, 446–457.

Huang, X., Zhang, G. and Herring, S. W. (1993). Alterations of muscle activities and jaw movements after blocking individual jaw-closing muscles in the miniature pig. *Arch. Oral Biol.* **38**, 291–297.

Hylander, W. L. and Johnson, K. R. (1989). The relationship between masseter force and masseter electromyogram during mastication in the monkey *Macaca fascicularis*. *Arch. Oral Biol.* **34**, 713–722.

Hylander, W. L. and Johnson, K. R. (1997). *In vivo* bone strain patterns in the zygomatic arch of macaques and the significance of these patterns for functional interpretations of craniofacial form. *Am. J. Phys. Anthropol.* **102**, 203–232.

Hylander, W. L., Picq, P. G. and Johnson, K. R. (1991). Masticatory-stress hypotheses and the supraorbital region of Primates. *Am. J. Phys. Anthropol.* **86**, 1–36.

Jaslow, C. R. and Biewener, A. A. (1995). Strain patterns in the horncores, cranial bones and sutures of goats (*Capra hircus*) during impact loading. *J. Zool., Lond.* **235**, 193–210.

Lanyon, L. E. (1996). Using function loading to influence bone mass and architecture: objectives, mechanisms and relationship with estrogen of the mechanically adaptive process in bone. *Bone* **18** (Suppl. **1**), 37S–43S.

Mikic, B. and Carter, D. R. (1995). Bone strain gage data and theoretical models of functional adaptation. *J. Biomech.* **28**, 465–469.

Mosely, J. R. and Lanyon, L. E. (1998). Strain rate as a controlling influence on adaptive modeling in response to dynamic loading of the ulna in growing male rats. *Bone* **23**, 313–318.

Rafferty, K. R. and Herring, S. W. (1999). Craniofacial sutures: Morphology, growth and *in vivo* masticatory strains. *J. Morph.* **242**, 167–179.

Teng, S., Choi, I. N. W., Herring, S. W. and Rensberger, J. M. (1997). Stereological analysis of bone architecture in the pig zygomatic arch. *Anat. Rec.* **248**, 205–213.

Throckmorton, G. S. and Dechow, P. C. (1994). *In vitro* strain measurements in the condylar process of the human mandible. *Arch. Oral Biol.* **39**, 853–867.

Tonna, E. A., Singh, I. J. and Sandhu, H. S. (1984). Non-radioactive tracer techniques for calcified tissues. In *Methods of Calcified Tissue Preparation* (ed. G. R. Dixon), pp. 333–367. New York: Elsevier.

Zar, J. H. (1996). *Biostatistical Analysis.* Third edition. Town, NJ: Prentice-Hall Inc.